RANS SIMULATION OF COMBINED FLOW AND HEAT TRANSFER THROUGH OPEN-CELL ALUMINUM FOAM HEAT SINK

assistant professor Petre OPRIŢOIU*

*Technical University of Cluj-Napoca, Departament of Infrastructure, str. Observatorului, nr.72-74, 400363, Cluj-Napoca, Romania, E-mail: petre.opritoiu@ggi.utcluj.ro

Abstract

Frequently, advanced electronics, optics, nuclear equipment and high frequency microwaves systems require cooling of some devices at a heat flux of about 5-30 MW/m^2. To meet this demand the porous medium of the heat exchangers has to be compressed thus the spherical particles are distorted and agglomerated.

The aim of this research is to study by simulation the effect of open cell aluminum foam on the heat transfer and pressure drop in cooling devices at the high heat fluxes. Heat transfer and pressure drop in an open foam heat exchanger, made of aluminum of different porosity (ε) and porous density (PPI), cooled by water were investigated numerically using CFD code Fluent and the results are presented.

Maximum fluid flow velocity used was 1.2m/s. The permeability (K) and form coefficient (c_F) varied from 2.52×10^{-10} m^2 and 1276 m^{-1} to 3.44×10^{-9} m^2 and 4731 m^{-1}, respectively. It was determined that the flow rate range influenced these calculated parameters.

Heat flux (q) up to 1.38 MW/m^2 was removed by using porous sample with porosity 60% (ε=0.608) and average pore diameter (d_p) 2.3mm. Under this simulating condition, the difference between the temperature of the wall and the bulk water did not exceed 63□C.

An estimate of heat sink efficiency using compressed aluminum foam for cooling high-power electronic devices was done. The results obtained in this study are relevant to engineering applications employing metal foams ranging from convection heat sinks to filters and flow straightening devices.

***Keywords**: simulation, pressure drop, flow characteristics, heat transfer performance.*

1. Introduction

The problem of dissipating high heat fluxes has received much attention due to its importance in applications such as open-cell aluminum foam heat exchanger, cooling of electronic equipment.

The most effective way of cooling is pumping liquid inside these devices through michrochannels of porous medium. The effects of fluid velocity, particle diameter, type of porous medium and fluid properties on the heat enhancement were investigated.

However the estimated maximal values of the heat flux dissipated does not exceed 1.38MW/m^2, at pressure drop 8.22bar and at a velocity 1.2m/s in a single phase water flow. Most of the theoretical models and numerical simulations used pore diameter (d_p) as one of the basic parameters for calculating both heat transfer and friction in the porous medium of cooling systems.

Experimental studies on the effect of compression and pore size variations on the liquid flow characteristics and heat transfer has been performed by Boomsma and Poulikakos [1].

They showed the compressed open-cell aluminum foam heat exchangers had thermal resistance (R_t) that were two or three times lower than the best commercially available heat exchanger, with the same pumping power (Ẇ).

2. Theory

Compression in the y direction is parallel to the airflow. Compression in the x direction is transverse to the airflow. The highest heat transfer coefficient ($\alpha_{eff.}$) was obtained with compression in the x or y directions. However, the highest pressure drop (ΔP) was obtained with compression in the x direction. High-pressure efficiency was obtained with both y, and equal x and y, compression. Compression in the y direction yields high heat transfer and moderate pressure drop. Equal x and y compression results in lower heat transfer and lower pressure drop, compared with y compression [2].

In this case a model for numerical simulation and practical calculation needs somewhat other approaches and require an extension of experimental base to provide the necessary background.

Open-cell aluminum foam was used as a porous medium in the model of heat sink. Applied porous media is manufactured from special grades of atomized metal powders. The initial powder particle size controls the pore size and distribution when sintered to a specified density.

The permeability (K) is related to the pore size (d_p) and pore distribution (PPI). Material properties such as thermal conductivity, thermal expansion and density are highly dependent on the porosity and generally decrease as porosity increases.

Table 1 gives an overview of the physical properties of all foams which were tested by simulation. 40 PPI foam, of two different initial porosities, one of 92% and the other of 95% were compressed by various factors from two to eight.

The first two digits of the foam's name designate the porosity of the foam in pre-compressed form. The second pair of numbers of the foam name signify the compression factor.

Table1. Compressed foam physical data(A) and uncompressed foam physical data(B)[1].

Foam	Compression	Name	Expected porosity [%]	Effective porosity [%]
Panel A				
5%	2	95–02	90.0	88.2
	4	95–04	80.0	80.5
	6	95–06	70.0	68.9
	8	95–08	60.0	60.8
8%	2	92–02	84.0	87.4
	3	92–03	76.0	82.5
	6	92–06	52.0	66.9
Panel B				
Foam	Pore diameter [mm]	Ligament diameter [mm]	Specific surface area [m^2/m^3]	Effective porosity [%]
10 PPI	6.9	0.40	820	92.1
20 PPI	3.6	0.35	1700	92.0
40 PPI	2.3	0.20	2700	92.8

To measure the actual values of the porosity, each compressed foam block was weighed, each compressed foam block was weighed, and based on the external measurements, an effective porosity was calculated and compared to an expected final porosity based on the foam's initial solid fraction initial and compression factor.

The expected porosity was based on the simple physical relation for a change in volume, where M is the compression factor (ratio of the original uncompressed foam block height to the final compressed height) and ε is the void fraction of the material($0<\varepsilon\leq 1$).

$$\varepsilon_{compressd} = 1 - M(1 - \varepsilon_{uncompressed}) \qquad (1)$$

Figure 1 shows the expected porosity of the compressed foams blocks as lines with the actual porosity measurements represented as points.

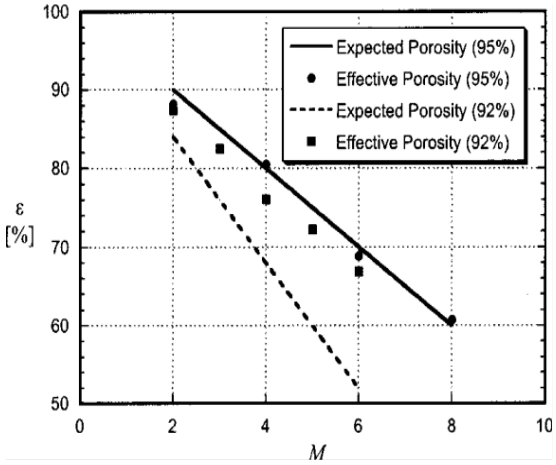

Fig. 1. The expected compressed metal foams porosities based on the precompression porosity and nominal compression factor compared against measured values [1].

The porosity of each block was calculated by dividing its weight by the volume, as measured by the external dimensions, and then comparing this value to the density of the solid material, aluminum 6101.

The surface aria to the volume ratio (specific surface aria) is also tabulated for the uncompressed metal foam blocks in Table 1. This specific surface area data were provided by the foam manufacturer [3].

Porous media model is nothing more than an added momentum sink in governing momentum equations. Since the volume blockage that is present physically is represented in the model, FLUENT uses and reports a superficial velocity inside the porous medium, based on the volumetric flow rate, to ensure continuity of the velocity vectors across the porous medium interface. The following properties are required [4]:

(a) *Porosity* (ε);

(b) *Viscous resistance* (1/K), for aluminum foam:

$$\frac{1}{K} = \frac{32\pi}{\varepsilon \times d_p} \qquad (2)$$

where K - permeability,[m^2] and d_p - pore diameter,[m];

(c) *Inertial resistance* (c_F)

$$c_F = \frac{2\left(\Delta P - \frac{vL\mu}{K}\right)}{v^2 \rho L} \qquad (3).$$

The theoretical pressure drop per unit length for porous media was predicted following Forchheimer equation (1901):

$$\frac{\Delta P}{L} = \frac{\mu}{K} \cdot \mathrm{v} + \frac{c_F}{\sqrt{K}} \rho \cdot \mathrm{v}^2 \qquad (4)$$

where $\Delta p/L$ - pressure drop per unit length, [Pa/m]; μ - fluid viscosity, [kg/m·s];K - permeability, [m^2]; v - velocity, [m/s]; c_F - innertial coefficient, [m^{-1}]; ρ - fluid density, [kg/m^3].

3. Results and discussion

3.1 Heat transfer performance

The final overall dimensions of the compressed foam blocks used in pressure-drop and heat transfer simulations were 240mm×100mm×100mm, with the cross-sectional area normal to the flow direction measuring 240mm×100mm.

To make them functional heat exchanger, each foam was brazed in a central position to an adjoining heat spreader plate made by solid aluminum.

A typical flow and heat transfer configuration is shown in fig. 2. A heat source is bonded or joined to a thin conductive substrate on which a block of open-cell aluminum foam of length L and thickness W is attached.

The foam is then placed in a channel, and cooling fluid of velocity u_0 at a temperature T_∞ is pumped through the open celled material, thereby affecting heat transfer from the hot source to the cooling fluid.

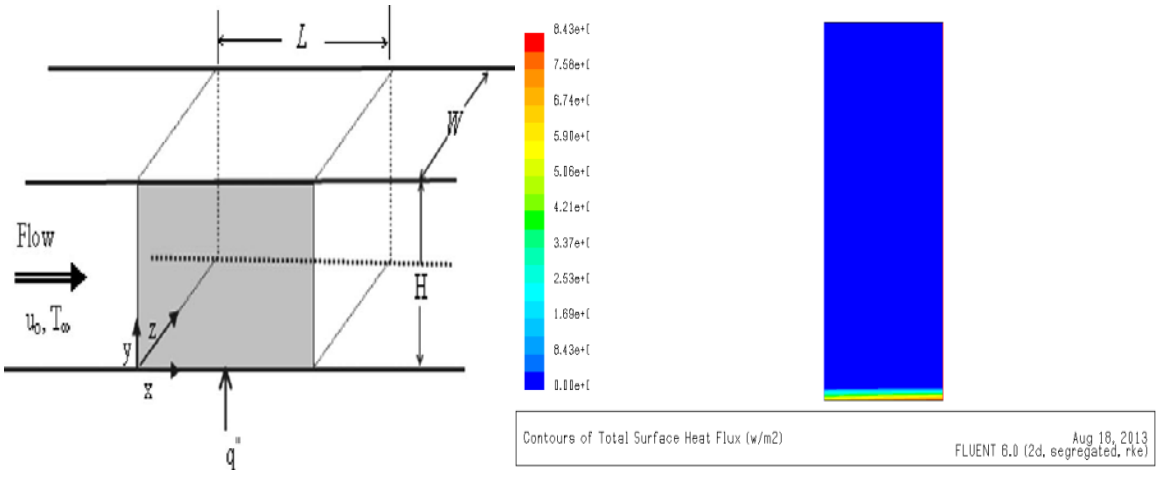

Fig. 2. Schematic of geometrical model as used in simulation [5] and contours of fluxes.

The heat transfer rate to the coolant q is defined by the following energy balance in eq. (5)

$$q = \dot{m}c(T_{out} - T_{in}) \qquad (5)$$

where T_{in}, T_{out} – the inlet and outlet temperature of the liquid, [K]; ṁ - mass flow rate, [kg/s] and c - specific heat, [j/kg·s]. Fig. 3 shows the value of the heat flux q, [MW/m^2] remove by the heat

exchanger of 10 cm thickness, depending on the velocity of the coolant. We can see that dissipation of heat flux up to 1.38MW/m^2 was obtained by simulation.

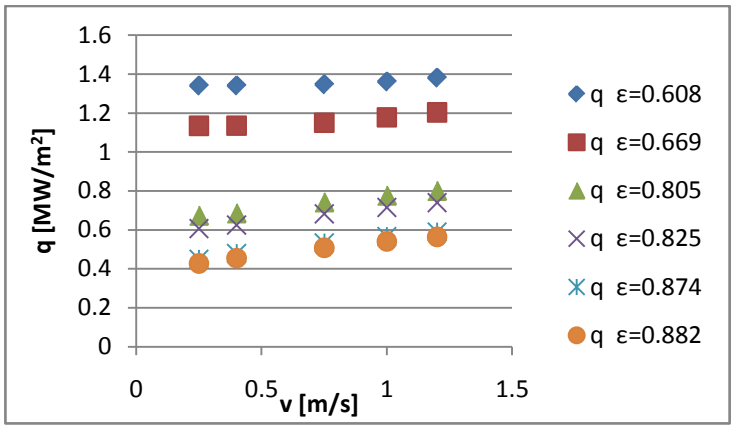

Fig. 3. Heat flux plotted against flow velocity

Under this simulating condition, the difference between the temperature of the wall and the bulk water did not exceed 63□C. A practical measure of the performance of a heat exchanging device is the dimensionless Nusselt number (Nu) as given in eq. (6).

$$Nu = \frac{\alpha_{por} \cdot d_l}{\lambda_f} \quad (6)$$

where α_{por}, [W/m^{2}K] is the convection heat transfer coefficient, which caracterizes the heat transfer between a solid and a fluid; λ_f, [W/mK] is thermal conductivity of the coolant and d_l, [m] is ligament diameter. The Nusselt numbers were calculated at various coolant flow rates and plotted against the coolant flow speed in fig. 4.

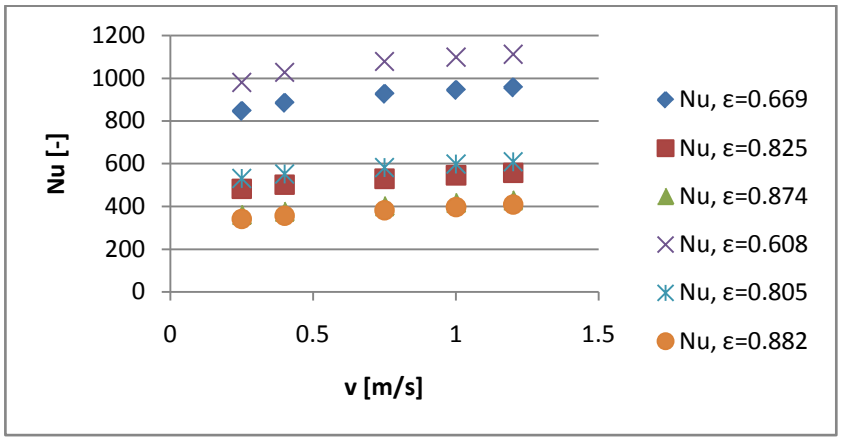

Fig. 4. Nusselt number plotted against flow velocity.

The heat transfer from the foam to the fluid will increase as either the porosity decreased (thus increasing surface area for heat transfer) or as the relative density (ρ%) increases (thus increasing heat conduction through the ligaments) or as the velocity of the fluid increases.

The localized heat transfer coefficient Nusselt (Nu) will vary with velocity, even at the low Reynolds number. This is primarily due to a physical phenomena caused by the tortuous nature of the porous flow.

At the openings between the cells, where the fluid passes from one cell to another, fluid passes through a contraction and expansion. At the back side of the opening (expansion side) the fluid develops eddies and vorticies. These vorticies will affect the mixing and local boundary layers, thereby affecting localized heat transfer from the cell walls to the fluid.

Heat transfer are commonly characterized by the Colburn factor (j), which gives a heat transfer performance estimate comparing the convection coefficient to the required flow rate of a heat exchanger. The Colburn factor is given in eq. (7) [7].

$$j = \frac{\alpha_{por}}{\rho c \mathrm{v}} \left(\frac{\nu}{a} \right)^{2/3} \quad (7)$$

where ν is the kinematic viscosity and a is the fluid thermal diffusivity. Fig. 5 show the value of the Colburn factor depending on the Reynolds number.

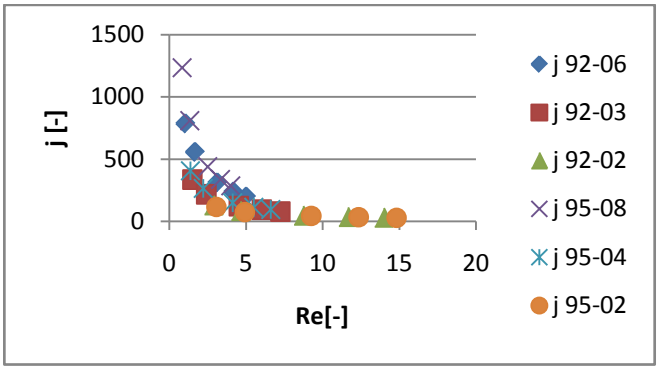

Fig. 5. Colburn factor plotted against permeability-based Reynolds number

The values of Colburn factor are highest for foam 95-08 with ε=0.608, at very low values of Re_K. The heat sink 95-02, with ε=0.882 shows lower magnitude of Colburn factor, but its observed for extended range of Re_K. Clearly that the metal foam with verry high initial porosity, even compressed, yields low Colburn values.

In any heat exchanger design, the heat convection performance of the heat exchanger must be weighed against the energy required to operate the system, which is the pumping power in this configuration. The required pumping power Ẇ, [w] was calculated for the aluminum foam heat exchanger at various coolant flow velocities, according to eq. (8).

$$\dot{W} = \Delta P \cdot \mathrm{Q_v} \quad (8)$$

where ΔP is the pressure drop across the aluminum foam heat exchager and Q_v, [m^3/s] is the volumetric flow rate of the coolant passing through the heat exchanger. Also, a common means to measure the heat convection effectiveness is the thermal resistance R_t, [K/w] as shown in eq. (9).

$$R_t = \frac{\Delta T}{q} = \frac{T_{pl} - T_{in}}{\dot{m} c (T_{out} - T_{in})} \quad (9)$$

where T_{pl} – average wall temperature. Lower thermal resistance facilitates the heat flow through heat exchanger (fig. 6).

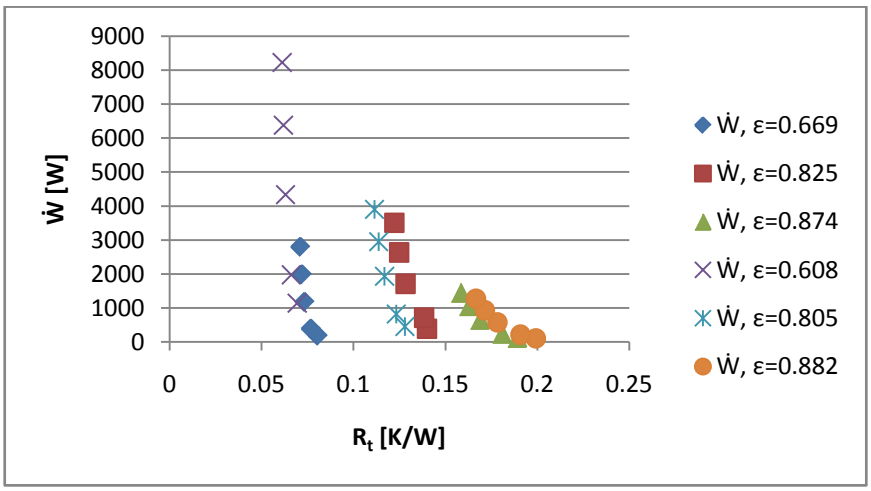

Fig. 6. Plot of the required pumping power against the corresponding thermal resistance.

In fig. 6 the optimal design is that which minimize the distance from the point to the origin of the plot. This point was obtain by foam 92-06 with porosity ε=0.669 and for a thermal resistance of 0.061K/W. The worst performance was generated by 95-02 with porosity ε=0.882 and for a thermal resistance of 0.199K/W. The metal foam heat exchangers decreased thermal resistance by nearly half when compared to currently used heat exchangers designed for the same application.

3.2 Pressure and flow characteristics

The amount of work required to pump the coolant through a heat exchanger is a critical heat exchanger design parameter. The parameters used to describe the pressure drop characteristics of the foam heat exchangers are the permeability and form coefficient which are defined in equation (4).

All data were calculated and reported on a Darcian flow velocity basis. This velocity accounts only for the channel dimensions, its independent of the porosity of the test material, and is practical for comparison against other sets of porous media. The range for the water velocities were from 0.25 to 1.2m/s and for pressure changes were from 0.113 to 8.226 bar.

Figure 7 shows the pressure drops simulating data and the fitted curves in graphical form for the compressed blocks based on velocity.

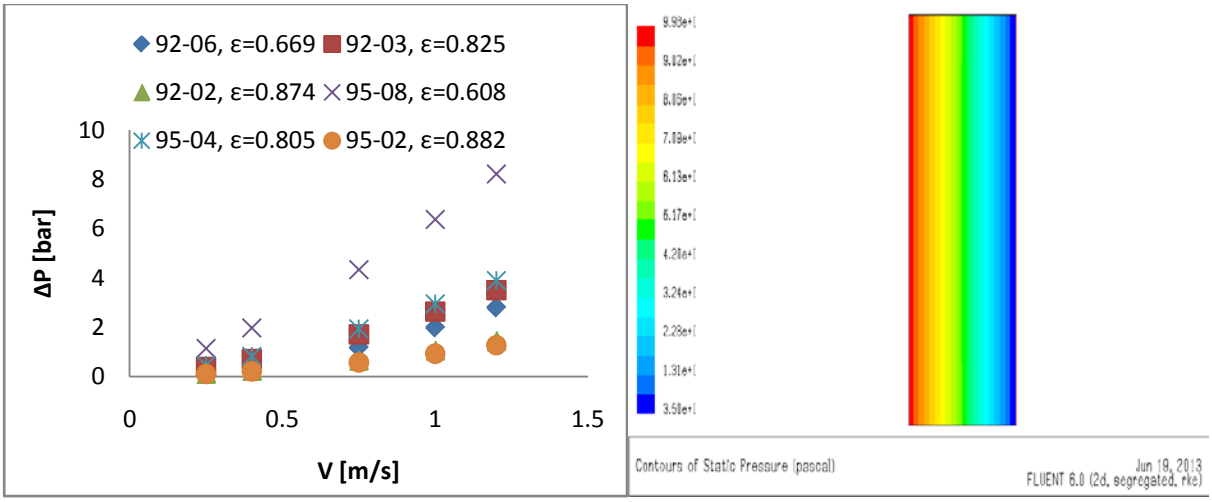

Fig. 7. Pressure drop versus fluid velocity for compressed foams and contours of static pressure.

As seen in fig. 7 compression has profound effect on the pressure-drop behavior of compressed foam. As expected, those foams which possess the highest solid fraction 95-08 (lowest ε) as seen in Table 1, generated the largest pressure drop. The foam which produced the lowest pressure drop was foam 95-02, which was also the most porous of the samples.

For a more general base of comparison, the hydraulic characteristics of the heat exchangers can be viewed using non-dimensional flow factors, like Reynolds number based on permeability (Re_K).

The characteristic length is replaced by the square root of permeability, as shown in eq. (10), where ρ is the density of the fluid, v is the Darcian flow velocity, and μ is the dynamic viscosity of the fluid.

$$\mathrm{Re}_K = \frac{\rho \mathrm{v} \sqrt{\mathrm{K}}}{\mu} \qquad (10)$$

The other commonly used non-dimensional flow describing factor is the Fanning friction factor (f) which is given in (eq.11). This provide information concerning the required pressure drop (ΔP) across a heat exchanger and come into use when the heat transfer performance to cost ratio is considered.

$$f = \frac{\Delta P}{4\left(\frac{L}{D_h}\right)\left(\frac{\rho\, \mathrm{v}^2}{2}\right)} \qquad (11)$$

In eq. (11), the hydraulic diameter (D_h) is described by eq. (12):

$$D_h = \frac{4A_C}{L_p} \qquad (12)$$

with A_C being the cross-sectional area of the flow channel and L_p being the wetted perimeter of the flow channel. Fig. 8 plots the friction factor of eq.(11) against the velocity. Refering to the friction factor the pressure drop of the foam is dominated by the form coefficient of eq. (4).

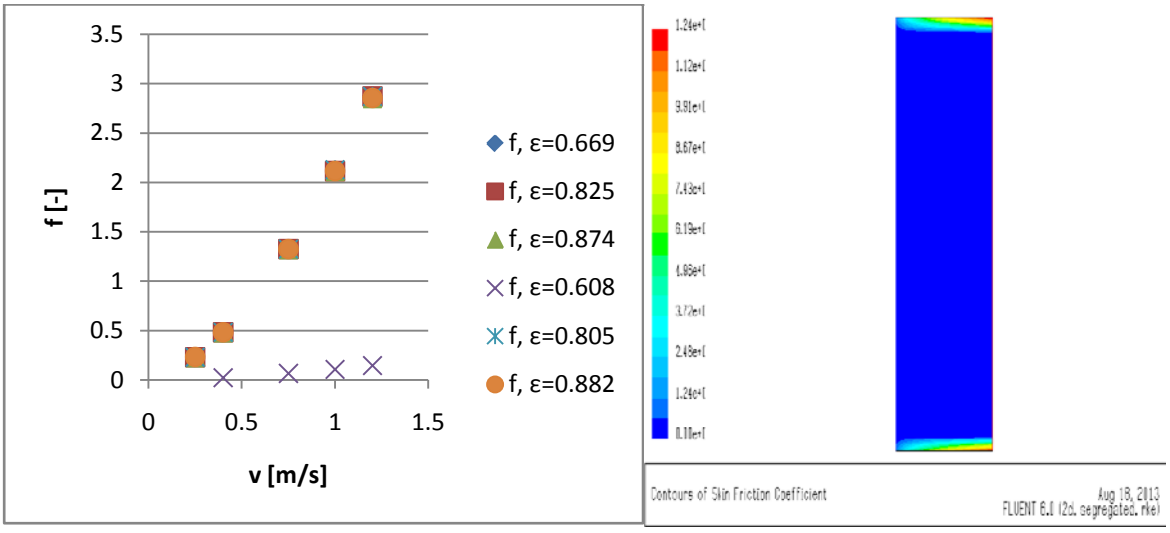

Fig. 8. Friction factor plotted against darcian velocity and contours of skin friction coefficient.

Permeability and form coefficient were calculated for each block using the entire flow rate range tested for each foam block (Table 2).

Table 2 Flow characteristics and associated pressure drop

Foam	ε[-]	K[m^2]	cF[1/m]	ΔP[bar]
95-08	0.608	2.52E-10	4731	1.149-8.226
92-06	0.669	3.95E-10	3399	0.180-2.800
95-04	0.805	6.87E-10	2957	0.461-3.905
92-03	0.825	8.26E-10	2820	0.393-3.503
92-02	0.874	3.08E-09	1472	0.128-1.457
95-02	0.882	3.44E-09	1276	0.113-1.274

Both foam samples series which were 95% and 92% porous before compression show similar flow behavior with the respect to the changes in the compression factor. For the 95% original porosity series, increasing the compression factor from two to four reduced the permeability from 3.44E-09m^2 to 6.87E-10m^2.

The other series of compressed foam blocks showed approximately the same sensitivity between the compression factor and the change in permeability.

Fig. 9 shows a plot of the permeability based on the measured porosity of the compressed metal foam samples. There is no difference made in the plotting data points between foams of 95% and 92% pre-compression porosity; all are placed on the same scale by their measured porosity in compressed form.

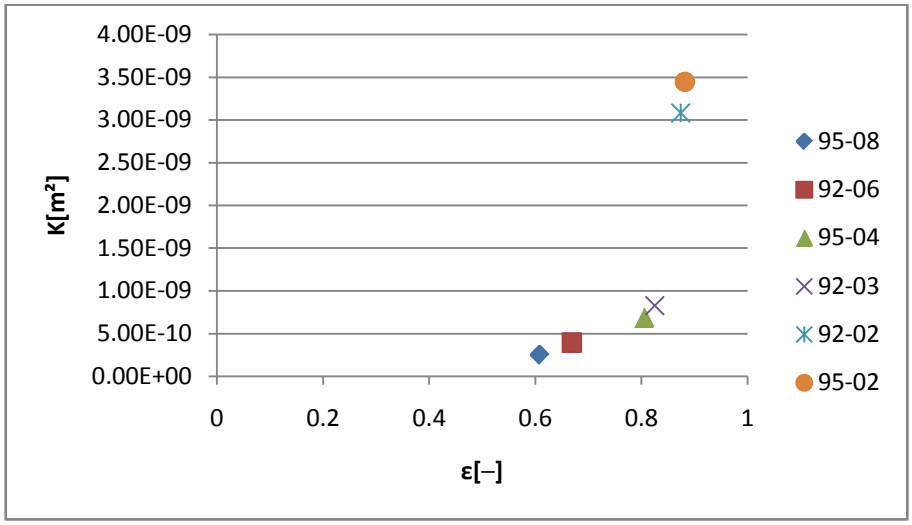

Fig. 9. The permeability of compressed foams is plotted against the values of measured porosity.

The form coefficient also varied with the compression of the metal foam blocks and the differing pre-compression porosities, ultimately being controlled by the porosity of the compressed metal foam. The form coefficient of the foams increased monotonically with decreasing porosity (fig. 10).

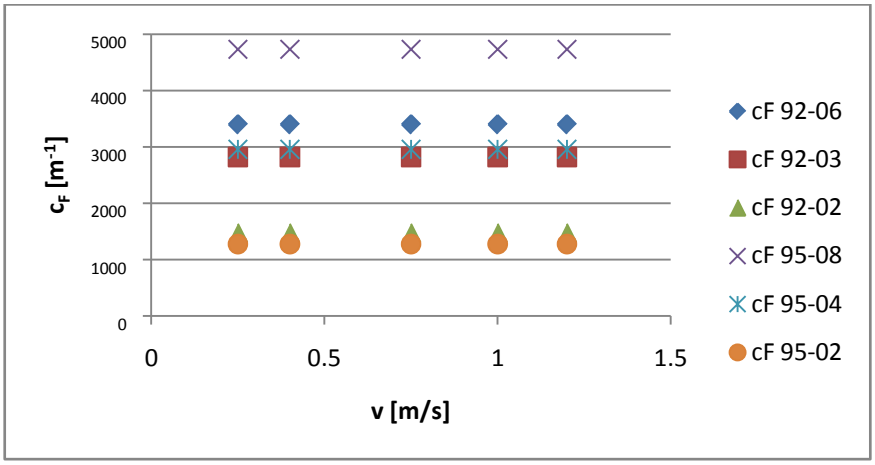

Fig. 10. The form coefficient of compressed foams is plotted against the darcian velocity.

The three aluminum foam blocks which were tested were of nearly the same porosity. The only difference between the samples was the average pore diameter. Referring to Table1, the porosities of these aluminum foam blocks ranged from 92% to 92.8%, and the pore diameter varied from an average of 6.9mm to 2.3mm. The difference in pore diameter appeared to dramatically affect the permeability and the form coefficient of the foams.

Decreasing the pore diameter (d_p), decreased the permeability and increased the form coefficient. The 10 PPI foam (95-02), which had a pore size of 6.9mm, generated the least flow resistance. In contrast, the 40 PPI foam (92-06) with a pore size of 2.3mm, had the greatest flow resistance. The increase of flow resistance directly relates to the effective surface length as explained by Lage [6], which relates an increase in drag to the increase in the specific surface area.

That values for the permeability and form coefficient of the porous medium depend upon the flow velocity range over which are they are calculated [7]. The permeability and form coefficient were calculated for each foam by varying the flow velocity range which the terms were calculated to investigate this dependence [1]. Fig. 11 plots the permeability based on an increasing flow speed. The permeabilities of the three uncompressed foams are nearly constant.

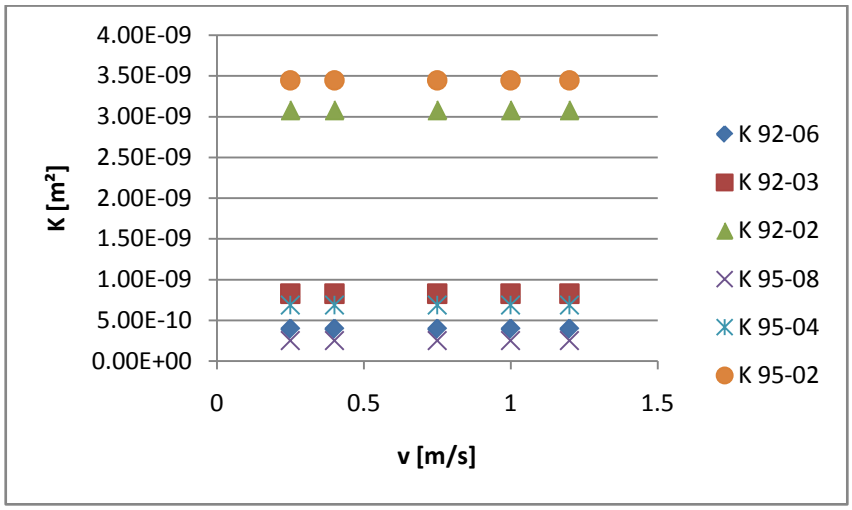

Fig. 11. Permeability plotted against darcian velocity

4. Conclusions about flow and heat transfer through open-cell foam

Open-cell aluminum foam compressed by various factors and then fashioned into heat exchangers for cooling electronic devices can dissipate large amounts of heats. Various heat exchanger evaluation methods were applied to the data, which included the hydraulic characterization, the heat transfer performance and an efficiency study to determine the most efficient metal foam heat exchanger configuration.

The compressed aluminum foam performed well not only in the heat transfer enhancement, but they also made a significant improvement in the efficiency over several commercially available heat exchangers which operate under nearly identical condition [8].

Open-cell aluminum foam were numerically tested to evaluate their hydraulic characteristics using water. The modules consisted of open-cell aluminum foams of various porosities and pore diameters.

The characterization procedure involved solving for two terms, the permeability and the form coefficient. These two factors accurately described the pressure-drop versus flow velocity behavior in porous media in general and were shown to be applicable to high porosity metal foams. From these simulations several conclusions can be drawn:

- The structural differences in the precompressed form did not a noticeable effect on the permeability. When comparing compressed foams with varying degrees of compression and initial porosities, the post-compression porosity governs the permeability and the resulting pressure drop.

- Increasing the compression factor decreased the permeability by regular amounts, which were nearly equal for of the two foam series (92 and 95%).

- The permeability of the compressed foams became more sensitive to changes in the porosity as the porosity increased.

- Holding the porosity constant and decreasing the pore diameter increased the flow resistance by reducing the permeability and increasing the form coefficient. This increase is attributed to the higher specific surface area generated by the smaller pore size.

- Using different flow velocity regimes resulted in various permeability and form coefficient values. Whenever the permeability and the associated form coefficient for a high-porosity porous medium are stated, the flow velocity range over which these terms are calculated must also be specified for accuracy.

REFERENCES

[1] Boomsma K. and Poulikakos D., 2002, The Effects of compresion and Pore Size variations on the liquid Flow characteristics in metal foams, ASME J. Fluids Eng., 124, pp. 263-272.

[2] John F. Klein, Noe Arcas, George W. Gilchrist, William L. Shields, Jr., Richard Yurman, and James B. Whiteside, 2005, Thermal Management of Airborne Early Warning and Electronic Warfare Systems Using Foam Metal Fins, Technology Review Journal.

[3] Duocel Aluminum Foam Data Sheet, 1999, ERG Material and Aerospace, Oakland.

[4] Opritoiu, P., 2007, Fluid flow and pressure drop simulation in aluminium foam heat exchanger, Acta Tehnica Napocensis, nr.50.

[5] Nihad, D., Ruben, P., and Alvarez, H., 2006, Heat transfer analysis in metal foams with low-conductivity fluids, ASME J. of Heat Transfer, 128, pp. 784-789.

[6] Lage J.L., 1998, The Fundamental Theory of flow through permeable media from Darcy to turbulence, Transport Phenomena in Porous Media, Elsevier Science, Oxford, pp.1-30.

[7] Antohe, B. V., Lage, J. L., Price, D. C., and Weber, R. M., 1997, Experimental Determination of Permeability and Inertia Coefficients of Mechanically Compressed Aluminium Porous Matrices, ASME J. Fluids Eng., 119, pp. 404-412.

[8] Boomsma, K., Poulikakos, D., Zwick, F., 2003, Metal foams as compact high performance heat exchangers. Swiss Federal Institute of Technology, Zurich, Switzerland.